DOI: 10.1002/ejic.201100371

Iron-Based Superconductors with Extended FeX_4 (X = As and Se) Tetrahedra

Ashok K. Ganguli*[a] and Jai Prakash[a]

Dedicated to Professor John D. Corbett on the occasion of his 85th birthday

Keywords: Iron / Pnictides / Chalcogens / Superconductors / Intermetallic compounds

Intermetallic compounds have been investigated over several decades for their interesting structural and physical properties, including magnetism and superconductivity. Among these, metal pnictides and chalcogenides of transition metals show diversity of bonding ranging from appreciable covalency to metal–metal bonds, which makes these compounds highly complex. ZrCuSiAs and $ThCr_2Si_2$ are of interest, because they provide an opportunity to design interesting intermetallics with tetrahedral layers exhibiting quasi-two-dimensional behavior. However, these metal pnictides and chalcogenides were not well known for their superconducting properties. The recent discovery of superconductivity at 26 K in a ZrCuSiAs-related structure (LaO/FFeAs) created huge excitement in the field of metal pnictide and chalcogenide superconductors. The role of the FeX_4 tetrahedra is significant for superconductivity. Distortion of the tetrahedra lowers the superconducting transition temperature (T_c) in these Fe-based superconductors. This article discusses the structural aspects of various new (2008–2011) families of Fe-based superconductors containing FeX_4 tetrahedra (X = As and Se) that act as charge carrier layers in these superconductors.

Introduction

Intermetallic compounds are known to exhibit several interesting properties like magnetism, superconductivity, hydrogen absorption, nuclear applications and shape memory.[1] Ternary transition metal phosphides with the general formula MM′P (M and M′ = transition metals) crystallizing in Fe_2P-type hexagonal structures are known in the literature.[2–5] Some of them show superconducting properties with maximum T_c values of 13 K for ZrRuP.[6] In 2008, the discovery of superconductivity at 26 K[7] in an arsenide (LaO/FFeAs) with ZrCuSiAs structure created huge excitement in the scientific community, and several new super-

[a] Department of Chemistry, Indian Institute of Technology, Delhi,
Hauz Khas, New Delhi 110016, India
Fax: +91-11-26854715
E-mail: ashok@chemistry.iitd.ac.in

Prof. Ashok K. Ganguli obtained his M. Sc. degree in Chemistry from the University of Delhi (1984) and his Ph. D. (supervisor: Prof. C. N. R. Rao FRS) from the Indian Institute of Science, Bangalore, India (1990). He then worked at the Central Research & Development Department of DuPont Company at Wilmington, Delaware, USA (1990–91), and Ames Laboratory, United States Department of Energy (USDOE) at the Iowa State University (1991–1993), where Prof. John Corbett FNASc (USA) introduced him to the fascinating world of polar intermetallics and Zintl phases and the finer aspects of crystal structure determination. In 1995, he joined the Department of Chemistry at the Indian Institute of Technology, Delhi. Prof. Ganguli has contributed extensively to the field of Solid State & Materials Chemistry, especially oxides (dielectric and superconducting), polar intermetallics (Zintl phases), and nanocrystalline materials. He has published around 150 papers in international journals and contributed 6 chapters in books. Prof. Ganguli is the recipient of the Materials Research Society of India Medal for 2006, the Chemical Research Society of India Medal for 2007, and he is a Fellow of the Indian Academy of Sciences. He is an Associate Editor of Bulletin of Materials Sciences and an Editorial Board Member of Indian J. Chem. A.

Mr. Jai Prakash obtained his B. Sc. (Hons) in Chemistry from the University of Delhi, India, in 2004. Later he obtained his M. Sc. in chemistry from the Indian Institute of Technology, Roorkee, with specialization in Analytical Chemistry in 2006. Currently he is working as a Ph. D. student at the Department of Chemistry, Indian Institute of Technology, Delhi, under the supervision of Prof. A. K. Ganguli on New Iron-Containing Oxypnictide Superconductors. He was awarded a travel grant by the International Center for Materials Research (ICMR), USA and Indian Institute of Technology, Delhi, to participate in the summer school at the University of California, Santa Barbara, USA, in 2009.

conductors with tetrahedral layers were discovered after this breakthrough. This review is focused on the structural aspects of recently discovered pnictide and chalcogenide superconductors with FeX_4 (X = As and Se) layers. These compounds are related to the PbFCl, ZrCuSiAs, and $ThCr_2Si_2$ structure types. We discuss the relation of the structures of newly discovered pnictide and chalcogenide superconductors and the role of the transition-metal-centered tetrahedra in enabling superconductivity.

LnOFeAs (Ln = lanthanide)

LnOFeAs (Ln = lanthanide) compounds were discovered by Jeitschko's group in 2000.[8] These compounds crystallize in the tetragonal ZrCuSiAs-type structure (space group: *P*4/*nmm*), which is a filled variant of the PbFCl (Matlockite) structure.[9]

A large number of inorganic compounds, which have a crystal structure similar to that of PbFCl, are known. PbFCl crystallizes in a primitive tetragonal structure (space group: *P*4/*nmm*), as shown in Figure 1. The structure of PbFCl could be understood as a cubic, close-packed-type structure of Pb atoms where Cl atoms occupy all the octahedral voids and F atoms occupy one-half of the tetrahedral voids in alternate layers. Pb and Cl atoms are present at the 2*c* crystallographic site [(0, 0.5, *z*), Z_{Pb} = 0.2 and Z_{Cl} = 0.65], while F atoms occupy the 2*a* crystallographic site (0, 0, 0).[10] The structure of PbFCl (AFX) can also be understood as parallel 011 layers of similar atoms, and the sequence of the layers is F-Pb-2Cl-Pb-F. The F atoms are connected with four Pb atoms in tetrahedral fashion. These $FPb_{4/4}$ tetrahedra are distorted and connected to each other in edge-sharing fashion. The Pb–F–Pb angles, which are above and below the F plane are designated as *α*, while the remaining four Pb–F–Pb angles are designated as *β* (Figure 2).

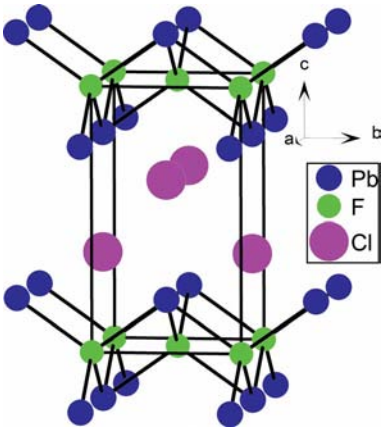

Figure 1. Crystal structure of PbFCl (space group: *P*4/*nmm*).

Angles *α* (109.67°) are slightly larger, and angles *β* (109.37°) are smaller than the ideal tetrahedral angle (109.5°)[11] in the structure of PbFCl (AFX). It should be noted that the *α* and *β* angles are related to each other. An

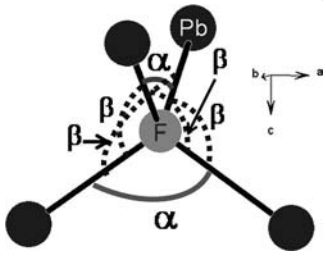

Figure 2. FPb_4 tetrahedra in the PbFCl structure (space group: *P*4/*nmm*).

increase in the size of X in an AFX-type structure induces a change in the structure from three-dimensional to layered.[12] For layered AFX structures, the interaction between XX layers is of the van der Waals type.[12] Half of the tetrahedral voids in this PbFCl (AFX) structure are vacant, which opens the possibility to derive new structures. The ZrCuSiAs structure (Figure 3) is obtained by filling the vacant halves of the tetrahedral voids (2*b* crystallographic sites) in the PbFCl structure.[9] Numerous compounds (more than 150) have a ZrCuSiAs-type structure, including the newly discovered LnOFeAs superconductors. The structure of LnOFeAs consists of alternate tetrahedral layers of Ln–O and Fe–As stacked along the *c* direction.

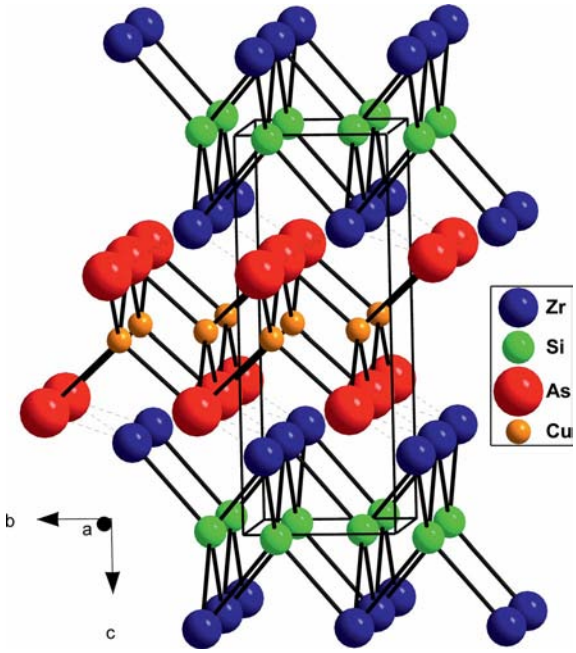

Figure 3. Crystal structure of ZrCuSiAs (space group: *P*4/*nmm*).

Both lanthanide and arsenic atoms occupy the 2*c* crystallographic site, while oxygen and iron atoms occupy the 2*a* and 2*b* crystallographic sites, respectively.[8] The Ln atoms (site symmetry: 4*mm*) form distorted square antiprisms with four arsenic and four oxygen atoms. The iron (site symmetry; $\bar{4}m2$) and oxygen atoms (site symmetry: $\bar{4}m2$) are tetrahedrally connected to four arsenic and four lanthanum atoms, respectively.[8] The [ZrSi] and [CuAs] tetrahedra in

ZrCuSiAs are elongated in the *c* direction with respect to LnOFeAs. Hence the Zr atoms in the [ZrSi] layer are close to the As atoms in the [CuAs] layer (2.8 Å), as shown in Figure 3. Also the [Ln–O] layers in LnOFeAs have ionic character, whereas the [ZrSi] layer in ZrCuSiAs shows strongly covalent character, which leads to the development of a polyanionic Si network (Figure 4).[9]

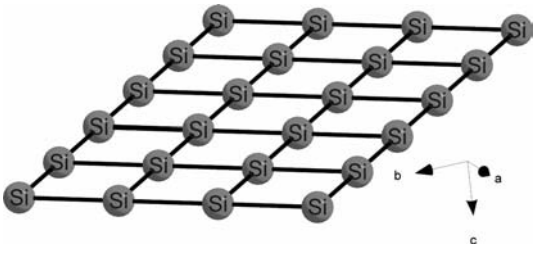

Figure 4. Si–Si network in ZrCuSiAs (space group: *P*4/*nmm*).

Si atoms are arranged in square planar fashion in ZrCuSiAs, as shown in Figure 4. The Si–Si distance in ZrCuSiAs is 2.598 Å. The Si–Si bonding and the interaction between the As and Zr atoms in ZrCuSiAs results in a three-dimensional covalent bonding network, while LnOFeAs compounds show two-dimensional character.[9]

The bonding between La and O in the [La–O] layer is ionic, whereas that in FeAs has predominantly covalent nature. Thus, the chemical formula of LaOFeAs may be expressed as $[LaO]^+[FeAs]^-$. The [Ln–O] layer acts as a charge reservoir, and the [Fe–As] layer acts as the conducting layer in LnOFeAs (Figure 5).[17] The charge carriers are confined in the two-dimensional [FeAs] layer. The distortion of $FeAs_4$ and $CuAs_4$ tetrahedra in LnOFeAs and ZrCuSiAs, respectively, results in two types of As–M–As (M = Fe or Cu) bond angle (discussed earlier). The α and β As–Fe/Cu–As angles in ZrCuSiAs and LaOFeAs are given in Table 1. The $CuAs_{4/4}$ tetrahedra in ZrCuSiAs are more distorted as compared to $FeAs_{4/4}$ tetrahedra in LaOFeAs (Table 1). The deviations from the ideal tetrahedral angle in ZrCuSiAs ($\beta - \alpha = 23.89°$) and LaOFeAs ($\alpha - \beta = 6.08°$) are much larger relative to those of $FPb_{4/4}$ tetrahedra in PbFCl ($\alpha - \beta = 0.3°$). The thickness of the FeAs layer (or CuAs in ZrCuSiAs) depends on the bond angle α. If α is large, then the FeAs layer is thinner. Therefore, the CuAs layer in ZrCuSiAs is much thicker than the FeAs layer in LaOFeAs.

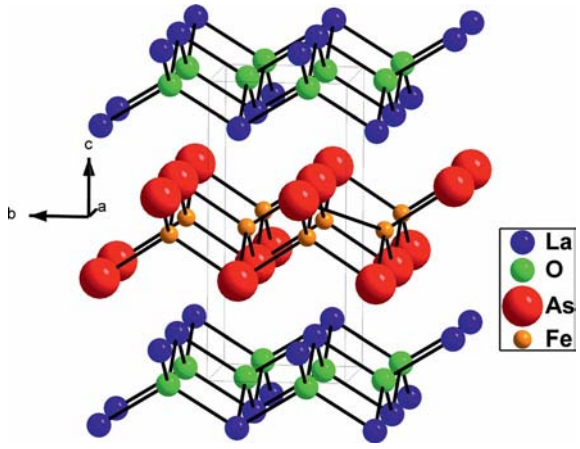

Figure 5. Crystal structure of LaOFeAs (space group: P4/*nmm*).

Table 1. Structural details of PbFCl, ZrCuSiAs, $ThCr_2Si_2$, and related compounds.

Composition	Lattice parameters		X–M–X angles	
	a [Å]	*c* [Å]	α [°]	β [°]
ZrCuSiAs*[9]	3.6736	9.5712	93.89	117.78 (X = As, M = Cu)
LaOFeAs*[8]	4.0353	8.7409	113.55	107.47 (X = As, M = Fe)
PbFCl*[11]	4.1060	7.2300	109.67	109.37 (X = F, M = Pb)
NaFeAs*[13]	3.9494	7.0396	108.27	110.07 (X = As, M = Fe)
β-$Fe_{1.01}Se$*[14]	3.7727	5.5260	103.98	112.29 (X = Se, M = Fe)
$ThCr_2Si_2$†[15]	4.0410	10.5870	112.72	107.87 (X = Si, M = Cr)
$BaFe_2As_2$†[16]	3.9625	13.0168	111.06	108.68 (X = As, M = Fe)

*space group: *P*4/*nmm*; †space group: *I*4/*mmm*

This has implications on the band structure and the electronic properties of these compounds. LnOFeAs compounds show structural transition from tetragonal to orthorhombic (space group: *Cmma*) at low temperatures (ca. 150 to 160 K).[18–20] Structural distortion from tetragonal (space group: *P*4/*nmm*) to orthorhombic symmetry (space group: *Cmma*) takes place below approximately 158[19] and 153 K[20] for CeOFeAs and PrOFeAs, respectively. Electronic calculations on LaOFeAs show that the energy bands near the Fermi level (E_F) originate from two-dimensional metallic sheets of Fe^{2+} ions.[21] There are 12 bands between –5.5 eV (relative to E_F) and –2.1 eV for LaOFeAs. These bands originate from O 2p and As 4p states; the As 4p contribution and As-derived bands are hybridized with the Fe 3d states. The extent of hybridization between Fe and As in LaOFeAs is comparable to that in oxides.[21] The bands near E_F are sensitive to the height of As from the Fe plane, which is controlled by the As–Fe–As bond angle.[21] In the low-temperature orthorhombic LnOFeAs structure, the $FeAs_{4/4}$ tetrahedra are more distorted as compared to those in the tetragonal form of LnOFeAs. There are three types of As–Fe–As angles in the orthorhombic structure of LnOFeAs[19–20] (Figure 6).

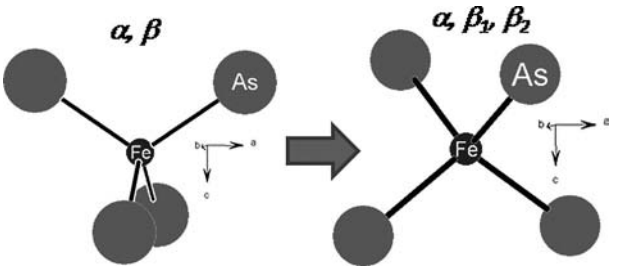

Figure 6. $FeAs_4$ tetrahedra in tetragonal CeOFeAs (space group:*P*4/*nmm*) (left) and orthorhombic CeOFeAs (space group: *Cmma*) (right).[19]

The α As–Fe–As angle (112.4°) in tetragonal CeOFeAs slightly decreases (112.17°) in the orthorhombic structure.[19] The β angle (108.03°), with a multiplicity of four in the tetragonal CeOFeAs structure, splits into two types of As–Fe–As angles (108.36° and 107.92°), each with a multiplicity of two.[19] The undoped LnOFeAs compounds are antiferromagnetic semimetallic in nature.[7] Introduction of holes or electrons through chemical substitution suppresses the antiferromagnetism and structural transition in these compounds with the evolution of superconductivity.[22–25] The doping of electrons through aliovalent substitution of O^{2-} by F^- in LnOFeAs induces superconductivity.[7,26,27] The substitution of O^{2-} by F^- leads to addition of electrons, which is confirmed by Hall and thermopower studies. The superconducting transition temperature (T_c) increases on isovalent substitution of smaller and heavier lanthanides in F-doped LnOFeAs (Figure 7), which reduces the lattice parameters (a and c) and corresponds to exerting a chemical pressure that changes the band structure and T_c of these compounds.[22,23,25–31] The maximum T_c achieved so far in these oxypnictides is 55 K[29] in the Sm(O/F)FeAs superconductor.

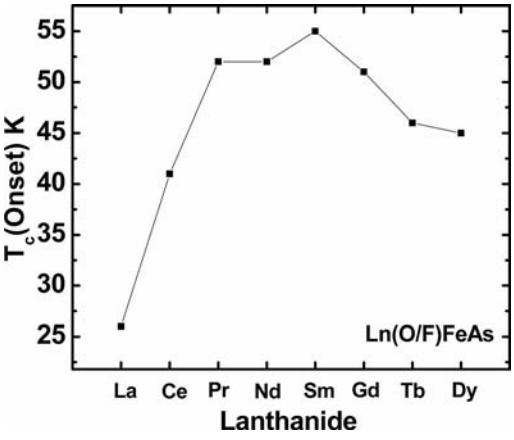

Figure 7. Variation of superconducting transition temperature (T_c) with lanthanide in Ln(O/F)FeAs. The values of T_c are taken from ref.[7] for La, ref.[26] for Ce, ref.[28] for Pr, ref.[23] for Nd, ref.[29] for Sm, ref.[30] for Gd, ref.[31] for Tb, ref.[31] for Dy.

Theoretical calculations by Jishi et al.[32] indicate that the charge transferred from the [Ln–O] layer to the [Fe–As] layer mainly resides on the As atoms. The substitution of oxygen by fluorine in LnOFeAs results in a transfer of electrons from the [Ln–O] layer to the [Fe–As] layer,[32] which strengthens the ionic bonding between the lanthanide and O/F atoms.[32] The enhancement in T_c from 26 to 43 K on application of pressure in $LaO_{0.9}F_{0.1}FeAs$ indicates that the superconductivity in these pnictides is unconventional.[17] The application of pressure on $LaO_{0.9}F_{0.1}FeAs$ leads to a systematic decrease in the lattice parameter c, which brings the [La-(O/F)] and [Fe–As] layers closer to each other, resulting in enhanced charge transfer from the [Ln–(O/F)] layer to the [Fe–As] layer.[25–32] The Fe–Fe distances in these LnOFeAs superconductors also play an important role in controlling the superconducting transition temperature (T_c). Qureshi et al.[33] have reported neutron diffraction studies on F-doped La(O/F)FeAs superconductors, which show that the T_c increases with decreasing Fe–Fe distance. Zhao et al.[19] also reported enhancement in T_c with decrease in Fe–Fe distance, which is directly related to the lattice parameter a [d(Fe–Fe) = $a/\sqrt{2}$].

Introduction of holes in LnOFeAs through substitution of Sr^{2+} at the lanthanide site also results in superconductivity with a maximum T_c of 25 K in (La/Sr)OFeAs.[34] Superconductivity in LnOFeAs can also be induced by doping of electrons directly in the FeAs layer by substitution of cobalt at the iron site,[35–37] with a maximum T_c of 15 K in $SmOFe_{0.9}Co_{0.1}As$.[37] The structural parameters along with the electron (or hole) concentration seem to be important in determining T_c. T_c in these pnictides is also dependent on the α and β angles in the $FeAs_4$ tetrahedra, and the ideal tetrahedral angle (109.5°)[19,38] leads to high T_c. This suggests that the $FeAs_4$ tetrahedra in these pnictides are very important for the superconducting properties.

AFe_2As_2 (A = Ca, Sr, Ba)

A large number of compounds with the general formula AB_2X_2 (A = lanthanide, alkaline earth, alkali metal; B = transition metal or main group element and X = element of group 14 or 15 and occasionally of group 13), which adopt the tetragonal $ThCr_2Si_2$-type structure (space group: $I4/mmm$), are known.

The tetragonal $ThCr_2Si_2$-type structure consists of tetrahedral layers of $CrSi_{4/4}$ separated by Th layers.[15] As in the ZrCuSiAs-type structure, the $CrSi_{4/4}$ tetrahedral units are edge-shared to form layers.[15] There are two tetrahedral $CrSi_{4/4}$ layers per unit cell, and these tetrahedra are distorted, which gives rise to two types of Si–Cr–Si angle, similar to those discussed earlier (α, β) (Figure 2). The α Si–Cr–Si angle (112.72°) is larger than the β angle (107.87°) in the $ThCr_2Si_2$ structure, which is opposite to the trend observed for the As–Cu–As angle in ZrCuSiAs, where the α As–Cu–As angle (93.89°) is smaller than the β As–Cu–As angle (117.78°). The coordination around Th is eightfold with silicon atoms at the corners of a flattened cube. The Cr–Si bonds are strongly covalent in nature, while the longer Th–Si bonds indicate ionic interaction between Th and Si.[15] Recently discovered FeAs-based AFe_2As_2 (A = alkaline earth metal) superconductors adopt the $ThCr_2Si_2$-type structure. These AFe_2As_2 compounds consist of interspersed $[Fe_2As_2]^{2-}$ layers and A^{2+} cationic layers[39] (Figure 8). The A layer acts as charge reservoir and FeAs layer acts as charge carrier. Each Fe atom is bonded to four As atoms in tetrahedral fashion, and A atoms are connected with eight As atoms, resulting in square prism geometry (Figure 9).

In this structure, A, Fe, and As atoms are present at the 2a, 4d, and 4e sites, respectively. AFe_2As_2 compounds also have two types of As–Fe–As bond angles designated as α and β. Angle α increases as the size of alkaline earth metal increases, while angle β decreases with increasing ionic ra-

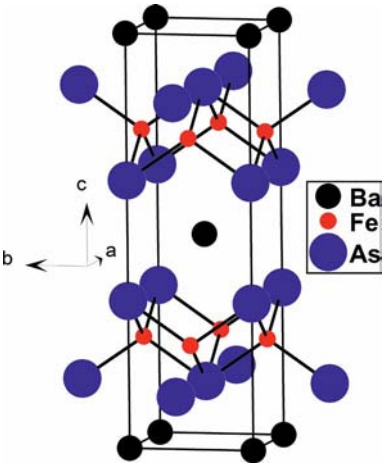

Figure 8. Crystal structure of $BaFe_2As_2$ (space group: *I*4/*mmm*).

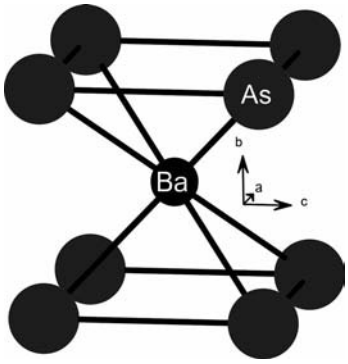

Figure 9. Ba and As connectivity in $BaFe_2As_2$ (space group: *I*4/*mmm*).

dius of the A metal ion in AFe_2As_2.[40–42] The α As–Fe–As angle is slightly smaller (111.06°) in $BaFe_2As_2$ as compared to the Si–Cr–Si angle (112.72°) in $ThCr_2Si_2$, which has a smaller β value than that of $BaFe_2As_2$. Similar to LnOFeAs, these AFe_2As_2 compounds also exhibit structural transition at low temperatures. Variable-temperature neutron diffraction studies on $BaFe_2As_2$[43] show a structural phase transition from a tetragonal (space group: *I*4/*mmm*) to an orthorhombic (space group: *Fmmm*) structure at approximately 142 K.[43] In the low-temperature orthorhombic structure of $BaFe_2As_2$, Fe forms distorted tetrahedra that give rise to three types of As–Fe–As bonds, each with a multiplicity of two. The structural transition in $BaFe_2As_2$ from tetragonal to orthorhombic leads to an increase in α, while β splits into two types, each with a multiplicity of two (108.80° and 108.15°). Iron atoms are arranged in a distorted square planar fashion in the orthorhombic AFe_2As_2 structure. Below the structural transition temperature (T_s), antiferromagnetic ordering of Fe moments takes place along the longer *a* axis. The magnetic moment of Fe in $BaFe_2As_2$ was found to be 0.87 μ_B per Fe atom[43] at 15 K, which is quite high as compared to that observed in LaOFeAs (0.36 μ_B per Fe atom).[18] The most striking difference between LnOFeAs and AFe_2As_2 compounds is that in the latter, the magnetic and structural transitions take place at the same temperature,[43] while in the LnOFeAs compounds, the structural transition takes place first, followed by ordering of iron magnetic moments[18–20] at much lower temperatures. The magnetic moments of iron are arranged in antiparallel fashion along the orthorhombic *a* and *c* axes, while they are parallel along the *b* axis. A large correlation length ($\leq$ 300 Å) indicates that the magnetic structure in $BaFe_2As_2$ has three-dimensional character and there is long-range antiferromagnetic ordering of Fe spins, despite the large interlayer distance between the neighboring Fe–As planes.[43] The Fermi surface and electronic structure of $BaFe_2As_2$ were calculated by Nekrasov et al.[44] within the local density approximation (LDA) with the linearized muffin-tin orbital (LMTO) method. The density of states (DOS) for $BaFe_2As_2$ was found to be flat, which supports the two-dimensional nature of this compound. The value of DOS for $BaFe_2As_2$ is similar to that of LaOFeAs at the Fermi level. The Fe 3d band width is larger (by 0.3 eV) for $BaFe_2As_2$ relative to that of LaOFeAs. The shorter Fe–As bonds in $BaFe_2As_2$ indicate a stronger Fe(3d)–As(4p) hybridization as compared to that in LaOFeAs.[44] The bands near the Fermi level are mainly contributed by Fe 3d orbitals.[44] The structural transition and antiferromagnetism associated with AFe_2As_2 compounds can be suppressed by doping of holes, similar to electron doping, in LnOFeAs, with evolution of superconductivity. Holes can be doped in AFe_2As_2 by replacing A^{2+} ions by K^+ ions; the resulting compounds show superconductivity with a maximum T_c of 38 K[40] in $Ba_{0.6}K_{0.4}Fe_2As_2$ (Table 2). Similar to LnOFeAs, superconductivity can also be introduced by direct doping of electrons in the FeAs layer through substitution of Co ions at the Fe site, with a maximum T_c of 22 K[45] in $Ba(Fe/Co)_2As_2$ (Table 2).

Table 2. Lattice parameters (*a* and *c*) and superconducting transition temperatures (T_c) of compounds of the type AFe_2As_2 (A = Ca, Ba, Sr, and Eu) (space group: *I*4/*mmm*).

Composition	Lattice parameters		T_c
	a [Å]	*c* [Å]	[K]
$Ca_{0.5}Na_{0.5}Fe_2As_2$[42]	3.829	11.862	20
$Ba_{0.6}K_{0.4}Fe_2As_2$[40]	3.917	13.297	38
$Eu_{0.5}K_{0.5}Fe_2As_2$[41]	3.867	13.091	32
$Eu_{0.7}Na_{0.3}Fe_2As_2$[46]	3.898	12.262	34.7
$Ba(Fe_{0.9}Co_{0.1})_2As_2$[45]	3.964	12.980	22
$Sr(Fe_{0.9}Co_{0.1})_2As_2$[47]	3.928	12.303	20

The application of pressure on these AFe_2As_2 compounds also induces superconductivity by suppressing the structural transition and antiferromagnetism. Neutron diffraction studies on single crystals of $CaFe_2As_2$ under high pressure reveal a transition from a tetragonal to a collapsed tetragonal structure.[48] These results show that superconductivity in these compounds is unconventional.[49] Superconductivity in AFe_2As_2-type compounds could also be induced by doping of electrons through substitution of trivalent lanthanide ions in place of divalent alkaline earth metals.[50,51] A maximum T_c of 47 K was observed in

$Ca_{1-x}Pr_xFe_2As_2$.[50] These lanthanide doped $CaFe_2As_2$ superconductors have higher transition temperatures as compared to their hole-doped analogues. The substitution of Pr^{3+} in $CaFe_2As_2$ results in a transition to a collapsed tetragonal (CT) structure along with doping of electrons.[51] The reduced lattice parameter *c* of lanthanide-doped $CeFe_2As_2$ could be playing an important role in enhancing the T_c as compared to hole-doped AFe_2As_2 superconductors. Similar to LnOFeAs superconductors, the maximum T_c in the AFe_2As_2 system was observed when the $FeAs_4$ tetrahedra were nearly ideal (tetrahedral angle: 109.5°).[38]

AFeAs (A = Li and Na)

The crystal structure for NaFeAs is shown in Figure 10. The AFeAs (A = Li and Na) compounds crystallize in the tetragonal anti-Cu_2Sb-type structure (space group *P*4/*nmm*), which is isotypic with the PbFCl structure.[11] The PbFCl (AFX) structure is made up of a sequence of fluorite slabs $[Pb_2F_2]$ separated by double Cl layers, as discussed earlier. In the anti-Cu_2Sb structure, the A atoms shift from the F sheet towards the X sheets, which results in square-pyramidal $[A_2X_2]$ slabs. In the Cu_2Sb structure, half of the copper atoms are connected with four Sb atoms in a tetrahedral fashion.[52] Similar to the PbFCl, ZrCuSiAs, and $ThCr_2Si_2$ structures, the $CuSb_{4/4}$ tetrahedra are edge-sharing and distorted, which gives rise to *α* and *β* Sb–Cu–Sb angles. The *α* Sb–Cu–Sb angle (95.05°) in Cu_2Sb is much smaller than *α* angles in the PbFCl, ZrCuSiAs, and $ThCr_2Si_2$ structures, while the *β* Sb–Cu–Sb angle (117.13°) is similar to the *β* As–Cu–As angle in ZrCuSiAs compounds.[52] In the AFeAs structure, Fe atoms occupy the 2*a* crystallographic site, while A and As atoms occupy 2*c* crystallographic sites. Its structure consists of layers of $FeAs_{4/4}$ tetrahedra in which Fe and As are arranged in anti-PbO-type layers (Figure 10).

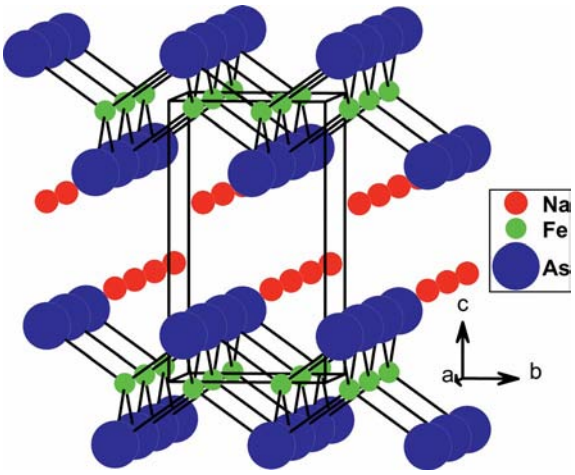

Figure 10. Crystal structure of NaFeAs (space group: *P*4/*nmm*).

α-PbO crystallizes in a tetragonal structure (space group: *P*4/*nmm*) consisting of edge-sharing tetrahedral layers of $PbO_{4/4}$ (distorted tetrahedral). The *α* O–Pb–O angles (118.17°), which are above and below the Pb plane, are larger than the *β* angles (105.30°).[53] The Fe–As tetrahedral layers in AFeAs are separated by a layer of A atoms, which are coordinated with As atoms (Figure 10). Edge-sharing $FeAs_{4/4}$ tetrahedra are distorted, which results in two types of As–Fe–As bond angles with multiplicities of two (*α*) and four (*β*), similar to the tetrahedra discussed earlier. The *α* angle (108.27°) in NaFeAs is smaller than the *β* angle (110.07°); this is opposite in trend to that observed in the PbO structure.[13,53] Variable-temperature neutron and X-ray diffraction studies of AFeAs show that these compounds do not undergo any structural transition at low temperature, and there is no evidence of antiferromagnetic ordering of iron spins. However, the theoretical calculations [local density approximation (LDA)] suggest that the Fermi surfaces and magnetic ordering in AFeAs are similar to those in LnOFeAs and AFe_2As_2. Transport and heat capacity studies by Chen et al.[54] on single crystals of $Na_{1-x}FeAs$ showed the presence of two anomalies at 52 and 41 K, which were assigned to structural and antiferromagnetic phase transitions, respectively. Muon-spin rotation (μSR) studies by Parker et al.[13] confirmed the antiferromagnetic ordering of Fe in NaFeAs. However, their studies do not show any evidence of structural transition. Li et al.[55] reported neutron scattering studies on single and polycrystalline samples of $Na_{1-x}FeAs$. Their studies reveal a transition from tetragonal (space group: *P*4/*nmm*) to orthorhombic structure (*Cmma*) near 50 K, which confirms the experimental observation of the structural transition at 52 K by Chen et al.[54] Thermal triple-axis spectroscopy on single crystals of $Na_{1-x}FeAs$ confirms the presence of an antiferromagnetic phase transition near 40 K.[54] $Na_{1-x}FeAs$ also forms a collinear in-plane antiferromagnetic spin structure similar to LnOFeAs and AFe_2As_2. The ordered magnetic moment of Fe was found to be 0.09 μ_B for NaFeAs, which is much smaller than those for undoped LnOFeAs and AFe_2As_2.[50] Nekrasov et al.[56] calculated the electronic structure of LiFeAs by the local density approximation (LDA) with the linearized muffin-tin orbital (LMTO) method.[56] Energy bands near the Fermi level originate from Fe 3d states (–2.5 to +2.5 eV), and As 4p states are lower in energy (–2.5 down to –6.0 eV) than iron states. The bandwidth of Fe 3d states in LiFeAs is larger, which results in lowering of the energy of As 4p states in LiFeAs as compared to LaOFeAs and $BaFe_2As_2$. The total value of DOS on the Fermi level (3.86 state/eV/cell) is slightly less than those for LaOFeAs (4.01 state/eV/cell) and $BaFe_2As_2$ (4.22 state/eV/cell).[56] Initial studies show that AFeAs compounds do not require doping of holes or electrons to induce superconductivity.[13,57,58] However some reports argue that there is some A ion deficiency, which results in hole doping in these AFeAs superconductors.[59]

The smaller value of the density of states on the Fermi level for LiFeAs may also be responsible for lower values of T_c (Table 3) in this superconducting compound, as compared to other iron-based pnictide superconductors.[56]

Table 3. Lattice parameters (a and c) and superconducting transition temperature (T_c) of AFeAs (A = alkali metals).

Composition	Lattice parameters		T_c
	a [Å]	c [Å]	[K]
LiFeAs[57]	3.776	6.357	16
NaFeAs[13]	3.949	7.039	9

β-FeS/Se/Te

β-FeS/Se/Te compounds crystallize in the tetragonal PbO-type structure (space group: *P*4/*nmm*), while α-FeSe crystallizes in the hexagonal NiAs-type structure, which is slightly iron-deficient ($Fe_{1-x}Se$). Fe atoms in β-FeSe are tetrahedrally connected to Se, and the $FeSe_4$ tetrahedra are distorted[60] similar to those in LnOFeAs, AFe_2As_2, and AFeAs, which gives rise to two types of Se–Fe–Se bond angle (α and β) (Figure 11). For $Fe_{1.01}Se$, the α Se–Fe–Se angle (103.98°) is smaller than the β angle (112.29°), which is opposite to the trend observed in the PbO structure. The interaction between the Se atoms of two adjacent FeSe layers is stronger as compared to the interaction between interlayers of oxygen atoms in the PbO structure.

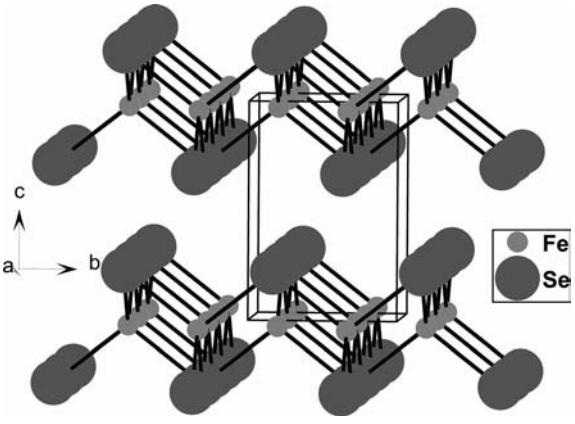

Figure 11. Crystal structure of β-FeSe (space group: *P*4/*nmm*).

Hsu et al.[60] discovered the superconductivity in the FeSe system, and they attributed the superconductivity to selenium deficiency ($FeSe_{0.82}$, T_c = 8 K). Contrary to this first report of superconductivity in selenium-deficient $FeSe_{0.82}$, McQueen et al.[14] showed that the superconducting FeSe is much closer to the stoichiometric FeSe (not Se-deficient) and slightly iron-rich. Variable-temperature structural studies by McQueen et al.[14] show that $Fe_{1.01}Se$ undergoes a transition from tetragonal (space group: *P*4/*nmm*) to orthorhombic structure (space group: *Cmma*) below 90 K.[14] In the low-temperature orthorhombic structure, the FeSe tetrahedra are more distorted as compared to those in the tetragonal structure, which gives rise to three types of Se–Fe–Se bond angles each with a multiplicity of two. The Se–Fe–Se angles that are above and below the Fe–Fe planes (104.28°) are smaller than other Se–Fe–Se angles. Enhancement in T_c from 8 K to 37 K[61] in FeSe on application of pressure suggests unconventional superconductivity in these iron chalcogenide superconductors.

Comparison of Structural Parameters

In all the Fe-based compounds discussed here, LnOFeAs, AFe_2As_2, AFeAs, and FeSe, the distorted, edge-sharing $FeX_{4/4}$ (X = As and Se) tetrahedra are omnipresent. For AFe_2As_2 compounds, two Fe–As layers are present in one unit cell, while other LnOFeAs, AFeAs, and FeSe compounds have one FeX (X = As, Se) unit per unit cell. The lattice parameter a of LnOFeAs, AFeAs, and AFe_2As_2 compounds are similar, but the lattice parameter c is quite different among these three FeAs-based families mainly because of the change from the primitive to the body-centered tetragonal cell. The lattice parameter c (13.0168 Å for $BaFe_2As_2$[16]) is largest in AFe_2As_2, while AFeAs compounds have the shortest lattice parameter c (6.3567 Å in LiFeAs[59]) among all these Fe-based superconducting families. For LnOFeAs compounds, the lattice parameter c decreases on substitution of smaller lanthanides at the La site.[22–24] Similar decreases in the lattice parameter c were also observed on substitution of smaller alkaline earth metals at the A site in AFe_2As_2,[40–42] but in the AFe_2As_2 system, this decrease in the lattice parameter c (Δc) on introducing smaller ions at the A site is more pronounced as compared to that in the LnOFeAs system. The reduction in the lattice parameter c of the LaOFeAs and AFe_2As_2 systems is due to interaction between two As atoms, and in LnOFeAs only intralayer As–As interaction exists while in AFe_2As_2 both inter- and intralayer As–As interaction exists. The Fe–As distance is largest in LnOFeAs compounds among the three families (LnOFeAs, AFeAs, and AFe_2As_2), while the Fe–As distances in AFeAs and AFe_2As_2 compounds are similar.[13,40–42] Likewise, Fe–Fe bond lengths are longer in LnOFeAs compounds as compared to those in AFeAs and AFe_2As_2 compounds. The As–Fe–As bond angles are very important in these compounds, as the maximum superconducting transition temperature was achieved when the α As–Fe–As angle is close to the ideal tetrahedral angle (109.5°).[19,38] Also the extent of Fe–Fe bonding (Fe–Fe distance) is an important parameter for determination of superconducting properties; high T_c values in these Fe-based superconductors are obtained when the Fe–Fe distances are shorter.[33]

Conclusions

The occurrence of tetrahedral layers in several polar intermetallics, chalcogenides, and pnictides is frequently observed. We have discussed several structural aspects of the recent Fe-based pnictides and chalcogenides (LnOFeAs, AFeAs, AFe_2As_2, and FeSe) and compared them with the well-known PbFCl, ZrCuSiAs, and $ThCr_2Si_2$ structures. All these Fe-based pnictides and chalcogenides contain distorted, edge-sharing FeX_4 (X = As and Se) tetrahedra. Distortion of FeX_4 (X = As and Se) tetrahedra gives rise to two types of X–Fe–X angle (α and β), which are observed at room temperature in all the above pnictides and chalcogenides. At low temperature, the tetragonal LnOFeAs, AFe_2As_2, and β-FeSe compounds exhibit structural transi-

tion and antiferromagnetism. The structural transition in LnOFeAs, AFe_2As_2, and β-FeSe results in further distortion of the FeX_4 tetrahedra [three types of X–Fe–X angle (a, β_1, β_2)]. The doping of electrons/holes in LnOFeAs and AFe_2As_2 compounds suppresses structural transition and antiferromagnetism with evolution of superconductivity. The X–Fe–X angles have a strong bearing on superconductivity, as the maximum T_c is observed when the angles are close to the ideal tetrahedral angle (109.5°).

Acknowledgments

A. K. G. thanks the Department of Science and Technology (DST), Government of India, for financial support. J. P. thanks the Council of Scientific and Industrial Research (CSIR), Government of India, for a fellowship.

[1] a) N. S. Stoloff, C. T. Liu, S. C. Deevi, *Intermetallics* **2000**, *8*, 1313–1320; b) L. M. Schetky, *Mater. Res. Soc. Bull.* **1996**, *21*, 50–55.
[2] a) R. Fruchart, A. Roger, J. P. Sénateur, *J. Appl. Phys.* **1969**, *40*, 1250–1257; b) J. Roy-Montreuil, B. Deyris, A. Michel, A. Rouault, P. I'Hritier, A. Nylund, J. P. Sénateur, R. Fruchart, *Mater. Res. Bull.* **1972**, *7*, 813–826.
[3] A. Roger, J. P. Sénateur, R. Fruchart, *Ann. Chim. (Paris)* **1969**, *4*, 79–91.
[4] a) R. Guerin, M. Sergent, *Mater. Res. Bull.* **1977**, *12*, 381–388; b) J. P. Sénateur, D. Fruchart, D. Boursier, A. Rouault, J. Roy-Montreuil, B. Deyris, *J. Phys., Colloq.* **1977**, *38*, C7-61–C7-66.
[5] A. Mewis, *Z. Naturforsch., Teil B* **1979**, *34*, 14–17.
[6] H. Barz, H. C. Kut, G. P. Meisnert, Z. Fiskt, B. T. Matthias, *Proc. Natl. Acad. Sci. USA* **1980**, *77*, 3132–3134.
[7] Y. Kamihara, T. Watanabe, M. Hirano, H. Hosono, *J. Am. Chem. Soc.* **2008**, *130*, 3296–3297.
[8] P. Quebe, L. J. Terbuchte, W. Jeitschko, *J. Alloys Compd.* **2000**, *302*,70–74.
[9] V. Johnson, W. Jeitschko, *J. Solid State Chem.* **1974**, *11*, 161–166.
[10] V. Johnson, W. Jeitschko, *J. Solid State Chem.* **1973**, *6*, 306–309.
[11] B. G. Hyde, S. Andersson in *Inorganic Crystal Structures*, John Wiley & Sons, New York, **1988**, pp. 81–84.
[12] Y. R. Shent, U. Englischt, L. Chudinovskikht, F. Porscht, R. Haberkoms, H. P. Becks, W. B. Holzapfelt, *J. Phys. Condens. Matter* **1994**, *6*, 3197–3206.
[13] D. R. Parker, M. J. Pitcher, P. J. Baker, I. Franke, T. Lancaster, S. J. Blundell, S. J. Clarke, *Chem. Commun.* **2009**, 2189–2191.
[14] T. M. McQueen, Q. Huang, V. Ksenofontov, C. Felser, Q. Xu, H. Zandbergen, Y. S. Hor, J. Allred, A. J. Williams, D. Qu, J. Checkelsky, N. P. Ong, R. J. Cava, *Phys. Rev. B* **2009**, *79*, 014522.
[15] J. Leciejewicz, S. Siek, A. Szytuea, *J. Less-Common Met.* **1988**, *144*, L9–L13.
[16] M. Rotter, M. Tegel, D. Johrendt, I. Schellenberg, W. Hermes, R. Pöttgen, *Phys. Rev. B* **2008**, *78*, 020503.
[17] H. Takahashi, K. Igawa, K. Arii, Y. Kamihara, M. Hirano, H. Hosono, *Nature* **2008**, *453*, 376–378.
[18] C. R. Cruz, Q. Huang, J. W. Lynn, J. Li, W. I. Ratcliff II, J. L. Zarestky, H. A. Mook, G. F. Chen, J. L. Luo, N. L. Wang, P. Dai, *Nature* **2008**, *453*, 899–902.
[19] J. Zhao, Q. Huang, C. de la Cruz, S. Li, J. W. Lynn, Y. Chen, M. A. Green, G. F. Chen, G. Li, Z. Li, J. L. Luo, N. L. Wang, P. Dai, *Nat. Mater.* **2008**, *7*, 953–959.
[20] J. Zhao, Q. Huang, C. de la Cruz, J. W. Lynn, M. D. Lumsden, Z. A. Ren, J. Yang, X. Shen, X. Dong, Z. Zhao, P. Dai, *Phys. Rev. B* **2008**, *78*, 132504.
[21] D. J. Singh, M.-H. Du, *Phys. Rev. Lett.* **2008**, *100*, 237003.
[22] X. H. Chen, T. Wu, G. Wu, R. H. Liu, H. Chen, D. F. Fang, *Nature* **2008**, *453*, 761–762.
[23] Z. A. Ren, J. Yang, W. Lu, W. Yi, X. L. Shen, Z. C. Li, G. C. Che, X. L. Dong, L. L. Sun, F. Zhou, Z. X. Zhao, *Europhys. Lett.* **2008**, *82*, 57002.
[24] J. Prakash, S. J. Singh, S. Patnaik, A. K. Ganguli, *Europhys. Lett.* **2008**, *84*, 57003.
[25] J. Prakash, S. J. Singh, S. Patnaik, A. K. Ganguli, *J. Phys. Condens. Matter* **2009**, *21*,175705.
[26] G. F. Chen, Z. Li, D. Wu, G. Li, W. Z. Hu, J. Dong, P. Zheng, J. L. Luo, N. L. Wang, *Phys. Rev. Lett.* **2008**, *100*, 247002.
[27] J. Prakash, S. J. Singh, A. Banerjee, S. Patnaik, A. K. Ganguli, *Appl. Phys. Lett.* **2009**, *95*, 262507.
[28] Z. A. Ren, J. Yang, W. Lu, W. Yi, G. C. Che, X. L. Dong, L. L. Sun, Z. X. Zhao, *Mater. Res. Innovations* **2008**, *12*, 105–106.
[29] Z. A. Ren, L. Wei, Y. Jie, Y. Wei, S. X. Li, L. Z. Cai, C. G. Can, D. X. Li, S. L. Ling, Z. Fang, Z. Z. Xian, *Chin. Phys. Lett.* **2008**, *25*, 2215–2216.
[30] J. Yang, Z. C. Li, W. Lu, W. Yi, X. L. Shen, Z. A. Ren, G. C. Che, X. L. Dong, L. L. Sun, F. Zhou, Z. X. Zhao, *Supercond. Sci. Technol.* **2008**, *21*, 082001.
[31] J. W. G. Bos, G. B. Penny, J. A. Rodgers, D. A. Sokolov, A. D. Huxleyac, J. P. Attfield, *Chem. Commun.* **2008**, 3634–3635.
[32] R. A. Jishi, H. M. Alyahyaei, *New J. Phys.* **2009**, *11*, 083030.
[33] N. Qureshi, Y. Drees, J. Werner, S. Wurmehl, C. Hess, R. Klingeler, B. Büchner, M. T. Fernández-Díaz, M. Braden, *Phys. Rev. B* **2010**, *82*, 184521.
[34] H. H. Wen, G. Mu, L. Fang, H. Yang, X. Zhu, *Europhys. Lett.* **2008**, *82*,17009.
[35] J. Prakash, S. J. Singh, S. Patnaik, A. K. Ganguli, *J. Solid State Chem.* **2010**, *183*, 338–343.
[36] A. S. Sefat, A. Huq, M. A. McGuire, R. Jin, B. C. Sales, D. Mandrus, L. M. D. Cranswick, P. W. Stephens, K. H. Stone, *Phys. Rev. B* **2008**, *78*, 104505.
[37] Y. Qi, Z. Gao, L. Wang, D. Wang, X. Zhang, Y. Ma, *Supercond. Sci. Technol.* **2008**, *21*, 115016.
[38] C. H. Lee, A. Iyo, H. Eisaki, H. Kito, M. T. F. Diaz, T. Ito, K. Kihou, H. Matsuhata, M. Brade, K. Yamada, *J. Phys. Soc. Jpn.* **2008**, *77*, 083704.
[39] E. Aktürk, S. Ciraci, *Phys. Rev. B* **2009**, *79*, 184523.
[40] M. Rotter, M. Tegel, D. Johrendt, *Phys. Rev. Lett.* **2008**, *101*, 107006.
[41] H. S. Jeevan, Z. Hossain, D. Kasinathan, H. Rosner, C. Geibel, P. Gegenwart, *Phys. Rev. B* **2008**, *78*, 092406.
[42] G. Wu, H. Chen, T. Wu, Y. L. Xie, Y. J. Yan, R. H. Liu, X. F. Wang, J. Ying, X. H. Chen, *J. Phys. Condens. Matter* **2008**, *20*, 422201.
[43] Q. Huang, Y. Qiu, W. Bao, M. A. Green, J. W. Lynn, Y. C. Gasparovic, T. Wu, G. Wu, X. H. Chen, *Phys. Rev. Lett.* **2008**, *101*, 257003.
[44] I. A. Nekrasov, Z. V. Pchelkina, M. V. Sadovskii, *JETP Lett.* **2008**, *88*, 144.
[45] A. S. Sefat, R. Jin, M. A. McGuire, B. C. Sales, D. J. Singh, D. Mandrus, *Phys. Rev. Lett.* **2008**, *101*, 117004.
[46] Y. Qi, Z. Gao, L. Wang, D. Wang, X. Zhang, Y. Ma, *New J. Phys.* **2008**, *10*, 123003.
[47] A. Leithe-Jasper, W. Schnelle, C. Geibel, H. Rosner, *Phys. Rev. Lett.* **2008**, *101*, 207004.
[48] A. Kreyssig, M. A. Green, Y. Lee, G. D. Samolyuk, P. Zajdel, J. W. Lynn, S. L. Bud'ko, M. S. Torikachvili, N. Ni, S. Nandi, J. B. Leão, S. J. Poulton, D. N. Argyriou, B. N. Harmon, R. J. McQueeney, P. C. Canfield, A. I. Goldman, *Phys. Rev. B* **2008**, *78*, 184517.
[49] T. Yildirim, *Phys. Rev. Lett.* **2009**, *102*, 037003.
[50] B. Lv, L. Z. Deng, M. Gooch, F. Y. Wei, Y. Y. Sun, J. Meen, Y. Y. Xue, B. Lorenz, C. W. Chu, **2011**, http://arxiv.org/ftp/arxiv/papers/1106/1106.2157.pdf.

[51] S. R. Saha, N. P. Butch, T. Drye, J. Magill, S. Ziemak, K. Kirshenbaum, P. Y. Zavalij, J. W. Lynn, J. Paglione, **2011**, http://arxiv.org/PS_cache/arxiv/pdf/1105/1105.4798v1.pdf.
[52] J. Nuss, M. Jansen, *Z. Anorg. Allg. Chem.* **2002**, *628*, 1152–1157.
[53] B. G. Hyde, S. Andersson in *Inorganic Crystal Structures*, John Wiley & Sons, New York, **1988**, pp. 261–262.
[54] G. F. Chen, W. Z. Hu, J. L. Luo, N. L. Wang, *Phys. Rev. Lett.* **2009**, *102*, 227004.
[55] S. Li, C. Cruz, Q. Huang, G. F. Chen, T. L. Xia, J. L. Luo, N. L. Wang, P. Dai, *Phys. Rev. B* **2009**, *80*, 020504.
[56] I. A. Nekrasov, Z. V. Pchelkina, M. V. Sadovskii, *JETP Lett.* **2008**, *88*, 543.
[57] M. J. Pitcher, D. R. Parker, P. Adamson, S. J. C. Herkelrath, A. T. Boothroyd, R. M. Ibberson, M. Brunelli, S. J. Clarke, *Chem. Commun.* **2008**, 5918–5920.
[58] J. H. Tapp, Z. Tang, B. Lv, K. Sasmal, B. Lorenz, P. C. W. Chu, A. Guloy, *Phys. Rev. B* **2008**, *78*, 060505.
[59] X. C. Wang, Q. Q. Liu, Y. X. Lv, W. B. Gao, L. X. Yang, R. C. Yu, F. Y. Li, C. Q. Jin, *Solid State Commun.* **2008**, *148*, 538–540.
[60] F. C. Hsu, J. Y. Luo, K. W. Yeh, T. K. Chen, T. W. Huang, P. M. Wu, Y. C. Lee, Y. L. Huang, Y. Y. Chu, D. C. Yan, M. K. Wu, *Proc. Natl. Acad. Sci. USA* **2008**, *105*, 14262–14264.
[61] S. Medvedev, T. M. McQueen, I. A. Troyan, T. Palasyuk, M. I. Eremets, R. J. Cava, S. Naghavi, F. Casper, V. Ksenofontov, G. Wortmann, C. Felser, *Nat. Mater.* **2009**, *8*, 630–633.

Received: April 7, 2011
Published Online: August 9, 2011

